Tracking chemical alteration in magmatic zircon using rare earth element abundances

Elizabeth A. Bell[a,*], Patrick Boehnke[b,c,1], Melanie Barboni[a,2], T. Mark Harrison[a]

[a] Dept. of Earth, Planetary, and Space Sciences, UCLA, 595 Charles Young Dr. E, Los Angeles, CA 90095, United States of America
[b] Dept. of the Geophysical Sciences, 5734 South Ellis Avenue, University of Chicago, Chicago, IL 60637, United States of America
[c] Chicago Center for Cosmochemistry, Chicago, IL, United States of America

ABSTRACT

Trace elements in magmatic zircon provide a wealth of petrogenetic information about host magmas. However, they are susceptible to alteration through post-magmatic interaction with hydrothermal fluids. Trace element analyses can also be biased by the inadvertent inclusion of exotic materials, such as mineral or glass inclusions, in analyzed volumes of zircon. In order to screen out samples with altered chemical signatures, zircons with high, flat light rare earth element (LREE) patterns are typically considered to be altered. However, visual selection of such patterns is qualitative and does not address ambiguous cases. The light rare earth element index (LREE-I = Dy/Nd + Dy/Sm) provides an approach for quantitative screening for aqueous alteration and contamination of zircon by exotic materials and was used to assess secondary processes in the greenschist facies Jack Hills detrital zircon suite. However, in addition to aqueous alteration, the LREE-I is also sensitive to melt compositional evolution, and its applicability to alteration in settings other than the Jack Hills quartzite is thus far undetermined. We investigate igneous zircon populations from a variety of geologic settings that show evidence for alteration by contact metamorphism during magma intrusion and deuteric fluid interactions during pluton crystallization. In suites with a high proportion of texturally altered zircons, low LREE-I values are common and this parameter correlates well with other contamination indicators (based on the observed secondary phases deposited in the zircons during fluid flow). Filtering zircon trace element compositions based on the LREE-I appears to remove the majority of chemically altered zircon, in many cases revealing previously obscured magmatic signals.

1. Introduction

Zircon naturally includes a variety of trace elements that are sensitive to its formation environment. Crystallization temperatures of magmatic zircon can be inferred from Ti contents (Watson and Harrison, 2005; Ferry and Watson, 2007), magma oxygen fugacity can be inferred from the magnitude of the Ce anomaly (Trail et al., 2011), and the U/Yb ratio can be used to infer continental versus oceanic origins (Grimes et al., 2007) and relative magmatic water content (Barth et al., 2013). Various rare earth element (REE) ratios track mineral fractionation and assimilation in magma, such as plagioclase (Eu/Eu*) or hornblende (light REE/heavy REE, or LREE/HREE), among others (e.g., Hoskin and Schaltegger, 2003; Barboni et al., 2016). Although the utility of REE and other trace elements for determining the provenance of detrital zircons has been debated (e.g., Hoskin and

Ireland, 2000; Hoskin et al., 2000; Belousova et al., 2002a; Grimes et al., 2007, 2015; Burnham and Berry, 2017), trace elements in > 4 Ga zircon have been used to infer a variety of properties of the early crust (e.g., Harrison et al., 2017).

Because of the importance of zircon for understanding Earth's earliest evolution, it is crucial to understand the circumstances under which its various geochemical and geochronological information can be altered. Heating and hydrothermal alteration can induce Pb loss in zircon, but the very low diffusivity of Pb in zircon means that this is almost never accomplished by diffusion of Pb from the undamaged zircon lattice (Cherniak and Watson, 2001). Instead, thermally-driven recrystallization (e.g., Hoskin and Black, 2000) or interaction of fluid with radiation-damaged regions of the zircon lattice is usually responsible. Similarly, the very low diffusivities of REE and many other trace elements in zircon (Cherniak et al., 1997) means that

---

Table 1

Zircon samples investigated in this study. Further information on sample location and petrology is available in the supplementary materials. Error bars are 1 s.d. *whole-rock Rb-Sr age from Whitney et al. (1976); **zircon U-Pb age from Fokin (2003); *°zircon U-Pb ages from Bell et al. (2018); ^zircon U-Pb age from Walker et al. (2007). All zircon U-Pb ages by ion microprobe.

| Sample	Age (Ma)	Location	Rock type	Geologic setting	Zircon CL texture	Possible alteration mechanisms
Suites with overall altered zircon textures						
Stone Mountain granite	291 ± 7**	Appalachian Inner Piedmont	2-Mica granite	Collisional	Dark, homogeneous	Extensive deuteric fluid flow + regional metamorphism
Suck Mountain granite	727 ± 20**	Appalachian Blue Ridge	2-Mica granite	Anorogenic	Mostly patchy or homogeneous	Regional metamorphism
IG1, RG5, RG6	113 ± 6*^, 113 ± 13*^, 120 ± 19*^	Peninsular Ranges Batholith (San Jacinto), older series	Granite, quartz diorite, leuco-tonalite	Continental arc	Magmatic (40%) + patchy	Intrusion by later granitoids
Suites with mostly unaltered zircon textures						
IG2, RG1, RG3	100 ± 13*^, 101 ± 9*^, 101 ± 8*^	Peninsular Ranges Batholith (San Jacinto), younger series	Tonalite, granodiorite, granodiorite	Continental arc	Mostly magmatic (75%)	None expected
Spirit Moun-tain leuco-granite	~16^	Spirit Mountain batholith	Leucogranite	Continental rift	Magmatic (58%) + patchy	Deuteric fluids
Spirit Moun-tain granite	16 ± 2^	Spirit Mountain batholith	Granite	Continental rift	Mostly magmatic (73%)	Intrusion by later granitoid; perhaps fault-related fluids
Mirage granite	15 ± 1^	Spirit Mountain batholith (Mirage pluton)	Granite	Continental rift	Mostly magmatic (92%)	Perhaps fault-related fluids

hydrothermal alteration likely outpaces diffusion as the primary means of trace element exchange in zircon. Because of their low concentrations, trace elements – especially the light rare earth elements – in zircon are vulnerable to dilution. This dilution may occur by either exotic materials introduced by hydrothermal alteration to the zircon during its residence in the crust, or by error in the laboratory, where mineral or glass inclusions in the zircon may be inadvertently introduced to the analyzed volume of host zircon. In situ methods allow some spatial specificity (e.g., Rubatto and Gebauer, 2000), which helps to reduce the danger of contamination by inclusions. However, hidden cracks or inclusions beneath the surface of the sample may still be inadvertently consumed during laser ablation or dissolved along with the zircon host during preparation for TIMS or solution ICP-MS analysis. Cryptocrystalline inclusions may also exist which are not visible to the analyst (cf. Cavosie et al., 2006). These materials, if inadvertently included in analyzed volumes of zircon, may significantly bias measured trace element abundances, obscuring magmatic and provenance histories.

Hydrothermal alteration of zircon imparts a characteristic high, flat pattern among the LREE relative to the middle REE (MREE) and HREE (e.g., Hoskin and Schaltegger, 2003). In many cases altered grains can be identified qualitatively, but the natural LREE/HREE ratio of magmatic zircon varies over a large range, making this distinction difficult for many cases. For example, while Hoskin (2005) used the La/Sm ratio and the concentration of La to discriminate magmatic versus hydrothermal zircon, many natural zircons fall in between these two categories on the La/Sm vs. La discriminant diagram (e.g., Bell et al., 2016). Bell et al. (2016) also attempted to define quantitative criteria for recognizing alteration, proposing the light rare earth element index (LREE-I = Dy/Nd + Dy/Sm) for tracking the raising and flattening that typically affects the LREE pattern due to either reaction with hydrothermal fluid or incorporation of exotic materials. For detrital zircons from the Jack Hills meta-conglomerate of Western Australia (e.g., Compston and Pidgeon, 1986), they proposed that LREE-I values > 30 represent unaltered magmatic zircon compositions, while values < 10 are affected by alteration or contamination by other phases. Indeed, below LREE-I = 30, the correlation of lower LREE-I values with increasing concentrations of P, Ti, Fe, and U appears to record the increasing influence of the alteration assemblage that fills cracks and voids in the zircons, which is made up largely of xenotime, Fe oxides, and minor monazite (Bell et al., 2015).

Despite its promising early results, the LREE-I has only been applied to the Jack Hills zircons, and whether it tracks alteration in other settings is as yet unclear. Due to changing lattice strain parameters (e.g., Blundy and Wood, 2003), it is likely that REE pattern shape may change with cooling and magmatic compositional evolution apart from any contamination by other phases. The criteria for recognizing altered zircon versus pristine magmatic zircon with naturally high LREE/MREE ratios, for example, are also unclear. In order to distinguish the competing effects of contamination and melt compositional evolution on the REE patterns (and specifically the proposed LREE-I) of magmatic zircon, we examine zircon from both a variety of granitoids that are interpreted to have been altered either due to intrusion of later magmas or hydrothermal activity, and zircon from granitoids lacking clear alteration mechanisms. These granitoids range from Neoproterozoic to Miocene, include examples of I-, A-, and S-type magma, and originate from continental arcs, continental rifts, and a collisional orogen. Two of these plutons (Stone Mountain and Suck Mountain in the southern Appalachian Piedmont and Blue Ridge provinces, respectively) underwent regional metamorphism after their formation.

In this paper, we address the behavior of REE patterns in zircon in various environments in order to determine the extent to which variation in LREE-I can be identified as resulting from alteration or contamination as opposed to magmatic compositional evolution and cooling. We also investigate how well the LREE-I correlates with other potential indicators of chemical alteration to zircon, including
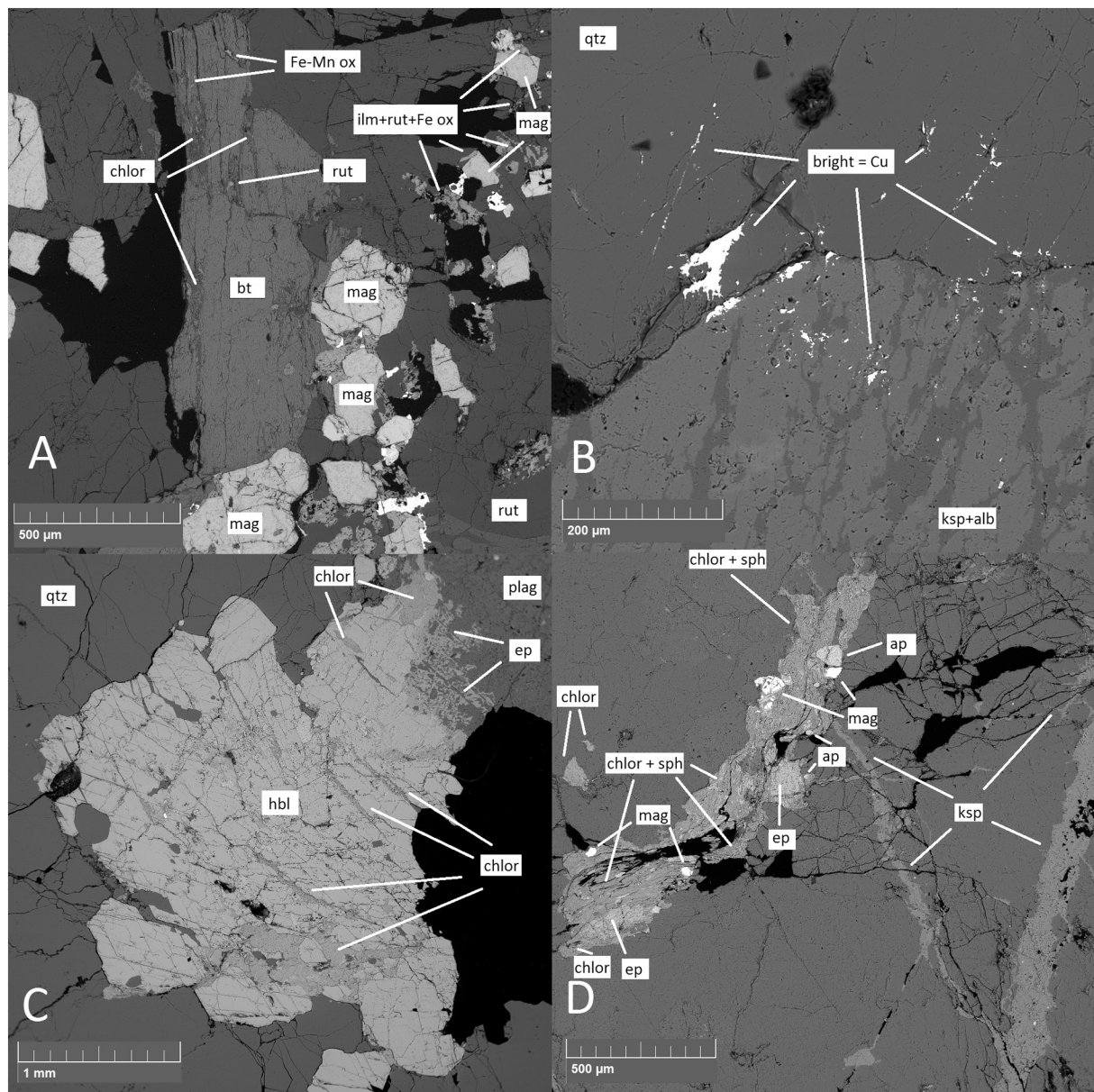
Fig. 1. Alteration features observed in thick section in various samples. A) Spirit Mountain leucogranite containing partially chloritized biotite; B) Spirit Mountain leucogranite containing Cu; C) hornblende in IG1 granite from San Jacinto Mountains older suite (subsequently intruded) partially replaced by chlorite and epidote; D) veins of K-feldspar and fine-grained intergrowths of chlorite + sphene associated with epidote in the Mirage granite (fault-related fluid flow).

disturbance to chemical zoning as shown by cathodoluminescence (CL) imaging, disturbance to the U-Pb isotopic system, and high abundances of elements associated with common contaminant phases such as P, Ti, and Fe (e.g., Geisler et al., 2003).

2. Samples and geologic settings

We analyzed zircon from granitoids from a variety of geologic settings, ranging in age from ~16 to ~730 Ma, with a variety of potential alteration mechanisms. Zircon suites range from those with textures that appear altered to those with mainly magmatic textures. Table 1 gives information on zircon suite texture, age, formation environment, and likely alteration mechanisms. Fig. 1 shows examples of alteration in thick section in representative samples, while Fig. 2 shows examples of zircon representative textures in cathodoluminescence imaging. Further information on location and description for each sample is given in electronic annex EA-1. Below, we include an overview of these samples

and the alteration mechanisms that likely operated on them, ranging from high to low temperature. Granitoids with no apparent mechanisms of alteration and largely zoned magmatic zircon are also included for comparison, along with a small number of inherited zircon cores.

2.1. Zircon suites with a high proportion of altered textures

2.1.1. Stone Mountain granite (sample StM)

The granite underlying Stone Mountain (Inner Piedmont, Georgia, USA) is a peraluminous, 2-mica granite (Wright, 1966) of S-type affinity (Chappell and White, 1974), emplaced during Alleghanian collision, with a whole rock Rb-Sr age of 291 ± 7 Ma (Whitney et al., 1976). The granite contains late aplite and pegmatite veins often ringed by skeletal tourmaline interpreted to indicate the expulsion of fluids during crystallization (Longfellow and Swanson, 2011). Since Alleghanian heating and deformation in the southern Appalachian Piedmont continued until at least 267 Ma (e.g., Dallmeyer et al., 1986; Hatcher Jr, 1987), the
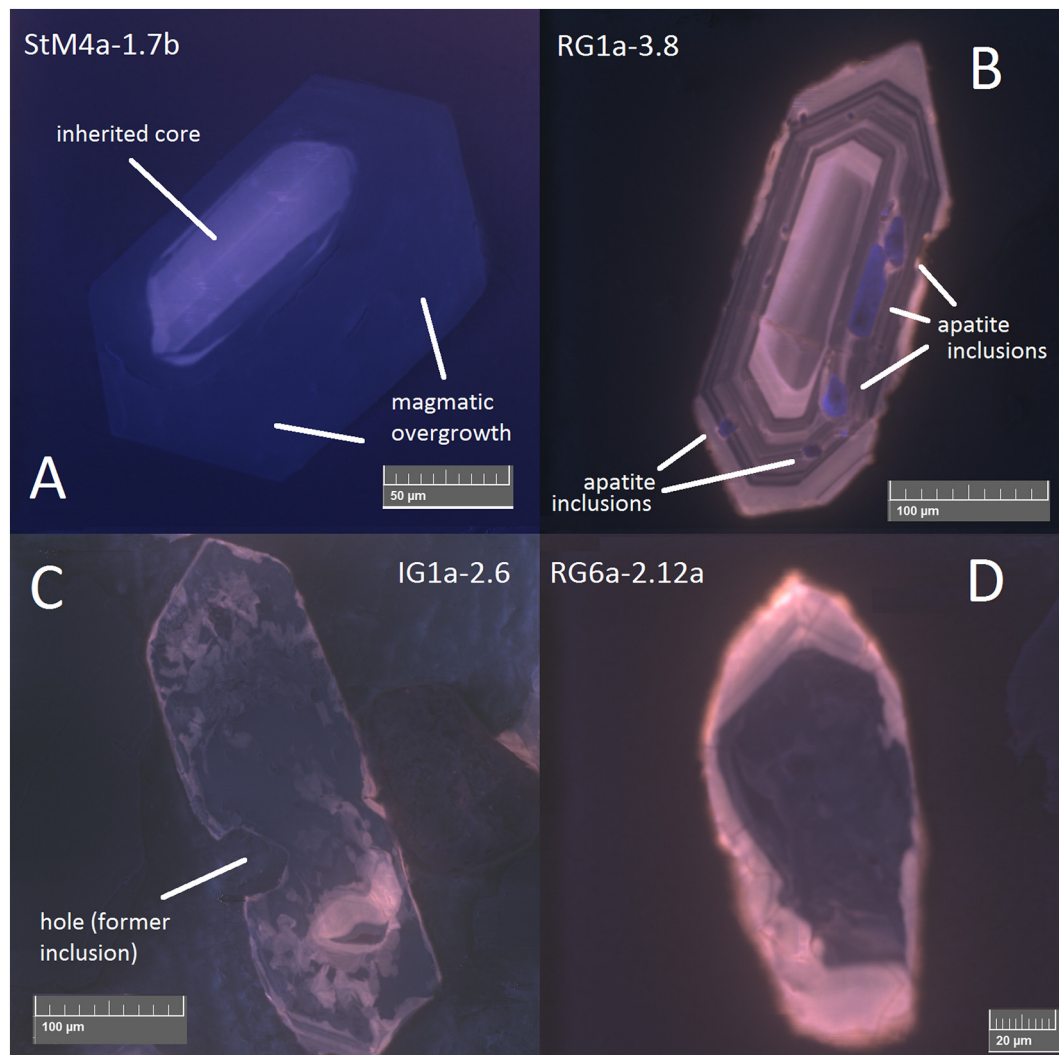
Fig. 2. Example CL textures showing various types of zoning in the sampled zircons. A) inherited core (bright) and Paleozoic magmatic overgrowth (dark, homogeneous) in the Stone Mountain granite; B) magmatic oscillatory zoning in a granodiorite from the youngest pulse of San Jacinto magmatism; C) patchy, alteration-related zoning in a granite from the older (subsequently intruded) suite of San Jacinto granitoids; D) replacement rims due to alteration in a leucotonalite from the older (subsequently intruded) suite of San Jacinto granitoids.

pluton may also have been affected by the ambient high crustal temperatures after its crystallization.

2.1.2. Suck Mountain granite (sample SuM)

The Suck Mountain granite (Peaks of Otter, Virginia, USA) is an A-type, 727 ± 20 Ma pluton (Fokin, 2003) intruded into the Virginia Blue Ridge, likely during the rifting that opened the Iapetus Ocean (e.g., Rankin, 1975; cf. Fokin, 2003). The 2-mica granite's whole-rock chemistry falls into the within-plate granite field (Pearce et al., 1984; Fokin, 2003). Although no one mechanism is suggested by outcrop relations, metamorphic fluid flow is likely to have occurred during the Paleozoic orogenies that affected the Blue Ridge province (e.g., Glover et al., 1982; Robinson, 1976; Sinha, 1976).

2.1.3. Older series from San Jacinto Mountains (granite IG1, quartz diorite RG5, leuco-tonalite RG6)

The San Jacinto Mountains are within the eastern zone of the Peninsular Ranges batholith (PRB) of southern California and are mostly underlain by several large bodies of tonalite and granodiorite with minor granite (Hill, 1984; Hill, 1988). Granite IG1 and quartz diorite RG5 are 113 Ma while leuco-tonalite RG6 is 120 Ma (Bell et al., 2018), corresponding to the older Santa Ana series of Hildebrand and

Whalen (2017). Many zircons from these samples have high common Pb contents and discordance (Bell et al., 2018). CL textures range from magmatic oscillatory zoning to patchy and mosaic-like, altered zoning (Bell et al., 2018).

2.2. Zircon suites with mostly magmatic textures

2.2.1. Younger series from San Jacinto Mountains (granodiorites RG1, RG3; tonalite IG2)

Our samples of the younger series of granitoids from the San Jacinto Mountains include granodiorites RG1 and RG3 and tonalite IG2. They derive from Hill's (1984) Units I and II of the San Jacinto pluton. These samples contain zircons with average U-Pb ages of ca. 100 Ma, but include scattered ages up to 110 Ma which may potentially be inherited from the older series of plutons into which these units intruded (Bell et al., 2018). CL textures range from magmatic oscillatory zoning to patchy and mosaic-like, altered zoning, but oscillatory zoning is the most common and is more widespread than in plutons of the older series (Bell et al., 2018).

2.2.2. Spirit Mountain leucogranite (sample SpLb)

The leucogranite of the Spirit Mountain batholith (southern

Nevada) formed from highly evolved melt in a continental rift setting (e.g., Haapala et al., 2005), which Walker Jr et al. (2007) interpreted as having been injected continuously into the upper regions of a long-lived magma chamber over 1–2 Ma. Walker Jr et al. (2007) identified vug cavities in the leucogranite related to late fluid circulation. We have identified small crystals of apparent native Cu in thick section in the leucogranite (see Fig. 1), likely formed by late-stage ore fluids. In addition, the mantling of euhedral magnetite crystals by Mn-rich ilmenite which shows extensive exsolution of rutile and Fe-rich ilmenite (see Fig. 1) also may point to late magmatic to subsolidus alteration.

2.2.3. Spirit Mountain granite (sample MG3b)

The Spirit Mountain granite is the main facies of the Spirit Mountain batholith of southern Nevada and is intruded by the Mirage Pluton on its eastern end (e.g., Haapala et al., 2005; Walker Jr et al., 2007). The Spirit Mountain granite was sampled both as pods included within the Mirage granite (MG3b/MGS1–5.x and MGS1-6.x of this study) and as a massive facies in contact with the Mirage granite (MGS2 of this study). Samples were identified in both cases by the porphyritic texture of the Mirage granite versus the local coarse equigranular texture of the Spirit Mountain granite (Walker Jr et al., 2007). The ages of the Mirage and Spirit Mountain granites cannot be distinguished by ion microprobe U-Pb dating (Walker Jr et al., 2007; Bell et al., 2018), and Walker Jr et al. (2007) interpret the Mirage granite to have intruded the Spirit Mountain batholith before the latter had fully solidified.

2.2.4. Mirage granite (sample MG3a)

The Mirage pluton intrudes the eastern end of the Spirit Mountain Batholith of southern Nevada (e.g., Haapala et al., 2005; Walker Jr et al., 2007). Although both the Mirage and Spirit Mountain granites are cut by later meter-scale diabase dikes (Walker Jr et al., 2007), none were present within several hundred meters of the Mirage granite sampling site in the present study. Some alteration to the rock is evident at the outcrop scale, with Walker Jr et al. (2007) noting stretched quartz crystals indicating subsolidus deformation. In thick section, we observe thin channels of secondary K-feldspar and patches of fine-grained, closely intergrown sphene and chlorite in association with epidote (see Fig. 2). Larger, euhedral sphene presumably of magmatic origin exists also in thick section, cross-cut by the late K-feldspar veins. The fine-grained intergrowths of sphene and chlorite are also seen filling cracks or inclusions in contact with cracks in zircon (Bell et al., 2018). It is possible that this chloritization occurred due to fluid flow along the nearby Davis Dam normal fault (Haapala et al., 2005; Walker Jr et al., 2007), which lies several tens of meters east of the sample site.

2.3. Known contaminating phases in the zircon suites

Most zircon suites in this study were previously characterized for mineral inclusion assemblages by Bell et al. (2018), with the exceptions being Suck Mountain granite (SuM) and Stone Mountain granite (StM). Preliminary searches for inclusions in the Stone Mountain granite identified monazite, xenotime, and U-Th silicates along cracks. Other zircon suites in this study share a similar inclusion character which is distinct from Stone Mountain zircons, with abundant apatite, variable contents of quartz, feldspar, ferromagnesian silicates, and clay minerals (Fig. 3). Clearly secondary phases fill cracks in some zircons (Fig. 3a), likely due to late-stage fluid circulation in the cooling plutons or potentially related to later hydrothermal alteration in the cases of the units cross-cut by later intrusions. These secondary phases are much richer in clay minerals, Fe-Ti oxides, epidote, and sphene than the phases either isolated from or in contact with cracks (Fig. 3c). Other than Stone Mountain, another exception to the general trend is the RG6 leuco-tonalite in the older pulse of San Jacinto granitoids, which has zircon relatively rich in micro-inclusions of U-Th silicates (Bell et al., 2018).

Apart from their much younger ages and less extensive history of

metamorphism, this suite of granitoid inclusions differs from that of the Jack Hills zircons in the much higher abundance of primary apatite (Bell et al., 2018; Rasmussen et al., 2011) as well as the much lower abundance of monazite and xenotime. Thus, it is likely that many of the phosphate-specific alteration and contamination effects identified in the Jack Hills zircons (Bell et al., 2016) may not hold universally true for in situ alteration of magmatic zircon and may be more common during the metamorphism of sediments.

3. Methods

Samples were crushed and sieved to < 425 μm. Following elution in water, heavy liquid and magnetic separation were used to concentrate zircon. Grains were mounted in epoxy and polished lightly with silicon carbide grinding paper to expose an interior surface. We used back-scattered electron and cathodoluminescence images taken on the Tescan Vega 3 scanning electron microscope at UCLA to find targets for SIMS analysis, while using EDS spectroscopy to characterize the mineral inclusion suites in the zircons. Magmatic zircon inclusion suites and/or U-Pb systematics for several of these samples (Spirit Mountain batholith and San Jacinto granitoids) were previously reported in Bell et al. (2018).

3.1. Analytical methods

U-Pb dating employed the CAMECA *ims*1270 ion microprobe at UCLA and was accomplished using a ca. 10 nA primary O$^-$ beam focused to a ca. 20 μm diameter spot. AS3 (Paces and Miller, 1993) was used as an age standard for calibration of the U/Pb relative sensitivity factor. Further details on this analytical method are available in Quidelleur et al. (1997).

Trace element analysis was also accomplished on the CAMECA *ims*1270 ion microprobe at UCLA with a ca. 15 nA primary O$^-$ beam focused to a ca. 30 μm diameter spot. Data were gathered at low mass-resolving power (~1000) with a −100 V energy offset to suppress molecular interferences. Relative sensitivity factor calibrations are based on analysis of NIST 610 glass standard, and the efficacy of the corrections was checked using the 91500 zircon standard (e.g., Wiedenbeck et al., 2004). Further details on the method can be found in Schmitt and Vazquez (2006).

3.2. LREE-I

The light rare earth element index (LREE-I; Bell et al., 2016), LREE-I = Dy/Nd + Dy/Sm (using concentrations rather than chondrite-normalized values) measures the changing of the LREE pattern in zircon as often recognized due to the presence of inclusions or fluid-assisted alteration (e.g., Hoskin and Schaltegger, 2003; Hoskin, 2005). LREE-I correlates with many other trace chemical parameters in detrital zircons from the greenschist facies Jack Hills meta-conglomerate including higher concentrations of P, U, Ti (the latter correlating to crystallization temperature) as well as an isotope of mass 57, dominantly ^{57}Fe, perhaps together with unresolvable interferences from molecular ions of Ca. This component is referred to as "Fe*" throughout the text. These observed contaminants to REE measurements in the Jack Hills zircons reflect the mineral assemblages filling cracks (and void space in contact with cracks) in the zircons: xenotime, Fe oxides, and monazite in addition to muscovite and quartz (Bell et al., 2015). It has been suggested (Bell et al., 2016) that breaks in slope between LREE-I and these contaminants at LREE-I = 30 likely represent the dividing line between zircon compositions dominated by alteration or contamination (LREE-I < 30) and unaltered magmatic zircon compositions (LREE-I > 30).

While it correlates with common contaminants, LREE-I also correlates with some expected indicators for magma compositional evolution in the Jack Hills zircons. With progressive cooling and mineral
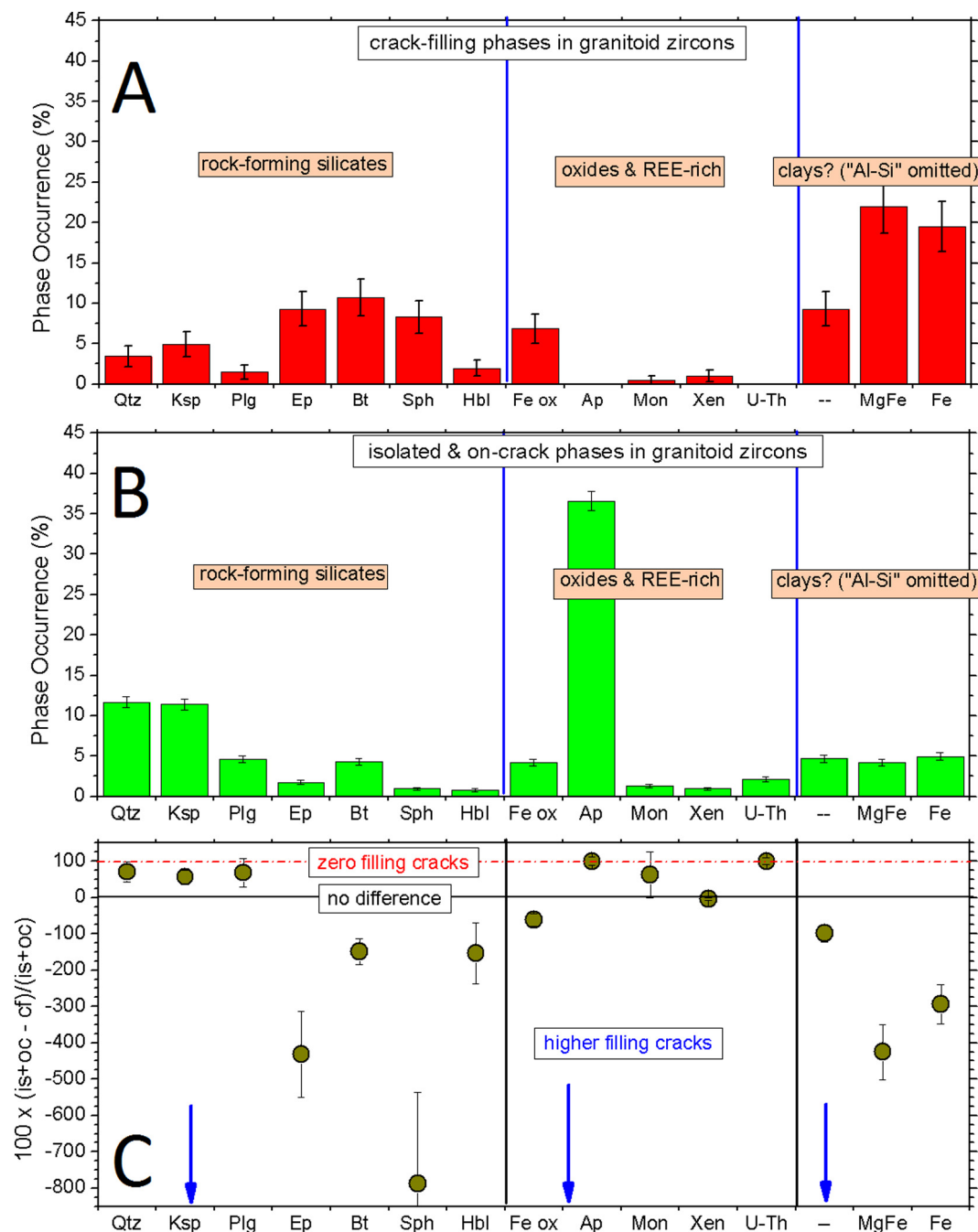
Fig. 3. Inclusion assemblages for granitoid zircons from this study and other rocks in the dataset of Bell et al. (2018). A) the clearly secondary assemblage that fills cracks; B) inclusions that do not take the shape of cracks and may be primary or secondary; C) the difference in occurrence rate between the inclusion and crack-filling assemblages. "–": samples with Al + Si evident in X-ray spectra.

fractionation in the magma, igneous zircon tends to increase in Hf and decrease in Th/U (Claiborne et al., 2010). Certain REE abundances and ratios related to mineral fractionation also vary systematically, such as a decrease in Eu/Eu* related to plagioclase fractionation and a decrease in HREE/MREE related both to changes in partitioning with cooling as well as the appearance of MREE-rich fractionating phases. This change in HREE/MREE slope is typically shown by the chondrite-normalized Yb/Gd ratio (e.g., Claiborne et al., 2010; Barth et al., 2013) and is also affected by the raising of the LREE during hydrothermal alteration, which may have a significant effect on Gd while having little effect on heavier MREE like Dy (Bell et al., 2016). For these reasons, we measure changes in HREE/MREE slope using the chondrite-normalized Yb/Dy ratio in order to minimize the effects of alteration.

4. Results

Most of the studied magmatic systems contain zircons that vary in LREE-I over one to three orders of magnitude (see Figs. 4–7). LREE-I correlates variably with indicators for melt evolution as well as potential contaminants and markers for disturbance to the U-Pb system. Geochronology and trace element data are collected in electronic annex EA-2.

4.1. Geochronology and LREE-I

While most samples show little correlation between LREE-I and discordance (Fig. 4a), the highly altered suites from Stone Mountain
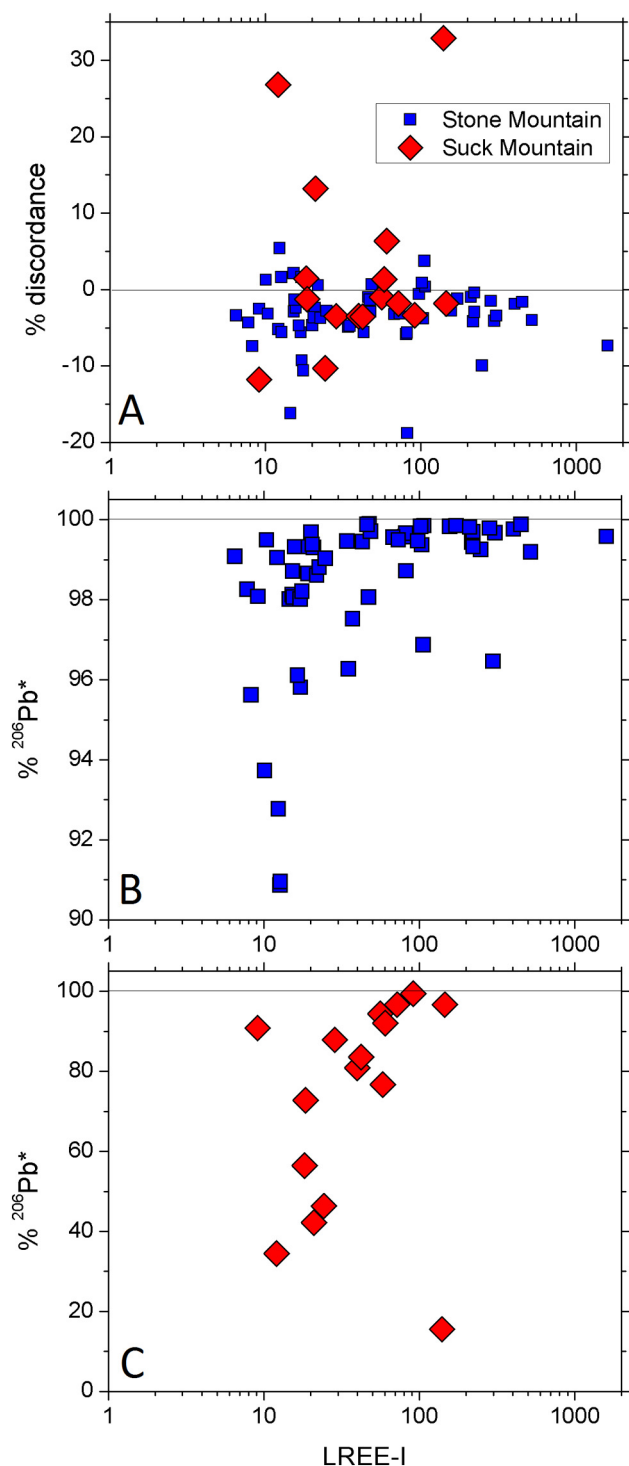
Fig. 4. Indications for disturbance to the U-Pb system vs LREE-I for several units in the study. In general, lower LREE-I is associated with common Pb contamination but shows less of a relationship with discordance. A) Zircons from Stone Mountain and Suck Mountain granites, discordance vs. LREE-I; B) percent radiogenic Pb versus LREE-I for Stone Mountain zircons; C) percent radiogenic Pb versus LREE-I for Suck Mountain zircons.

and Suck Mountain granites tend toward higher common Pb contents (typically resulting in lower radiogenic Pb) with lower LREE-I (Fig. 4b, c). U-Pb data from this study compare reasonably well with previously published ages for the Stone Mountain and Suck Mountain granites. Although the scatter in ages is high, magmatic overgrowths in the Stone Mountain zircons suggest an average age of 330 ± 40 Ma (1 s.d.), with

inherited cores ranging to 1360 Ma, compared to the 291 ± 7 Ma whole rock Rb-Sr age measured by Whitney et al. (1976) for the pluton. The high number of discordant grains we found in the Suck Mountain zircons are similar to the results of Fokin (2003). The 727 ± 20 Ma age of Fokin (2003) is similar to our age of 745 ± 35 Ma (1 s.d.) for the least contaminated, least discordant grains. San Jacinto granitoids show less coherent behavior between LREE-I and U-Pb systematics, with high common Pb values scattered throughout the range of LREE-I.

4.2. Zircon suites with a high proportion of altered textures (> 40%)

The three studied zircon suites containing mostly zircon with altered textures (Stone Mountain granite, Suck Mountain granite, and the older San Jacinto series) contain a high proportion of zircons with LREE-I < 30, with lower LREE-I values below 10. Stone Mountain (n = 85) and the older suite of San Jacinto zircons (n = 139) range over nearly three orders of magnitude in LREE-I, and the LREE-I correlates with light element contaminants (Fe*, Mn, Ti; see Figs. 5–6). The Stone Mountain zircons also show a negative correlation between LREE-I and Th/U below an LREE-I value of ca. 50, with no clear relationship at higher LREE-I. The Suck Mountain zircons (n = 23) range only an order of magnitude in LREE-I but show a similar proportion of values below 10.

Although most zircons with oscillatory zoning in the older San Jacinto suite have high LREE-I values, these apparently texturally unaltered zircons do range as low as LREE-I = 1 with magmatically untenable values (i.e., 1000s of ppm) of Ti, Mg, and Mn (see Watson and Harrison, 2005; Harrison et al., 2007). Only three out of the 23 analyzed Suck Mountain zircons display oscillatory zoning, ranging in LREE-I from 54 to 12 and with ambiguous levels of Mn and Ti). The relationship between LREE-I and light elements (Fe*, Mn, Ti) in both the Stone Mountain and older San Jacinto suites differs at low vs high LREE-I. The Suck Mountain suite (Fig. 5) does not show clear variations in behavior, potentially owing to the lower sample number (n = 23). For LREE-I > 50, Fe* and Mg are relatively low and show no relationship with LREE-I, whereas for LREE-I < 50, higher Fe* and Mg contents are increasingly found with lower LREE-I. The Fe* behavior is mirrored by Th/U, which also becomes far more scattered for LREE-I < 50, and HREE/MREE (reflected by Yb/Dy), which is dominated by lower values for LREE-I < 50 and flat for LREE-I > 50. The older San Jacinto zircons show less coherent trends in the light elements, but grains at LREE-I > 50–60 are tightly clustered with a fairly flat trend between LREE-I and the light elements Ti and Mn, with a more diffuse and slightly negative trend evident between LREE-I and these elements for LREE-I < 50.

Inherited zircon is common in the Stone Mountain granite, with ubiquitous CL-bright inherited cores typically displaying irregular, convoluted CL zoning. Rare Precambrian zircon cores are also inherited into the older and younger San Jacinto suites. Interestingly, most inherited cores retain high LREE-I values and, in the case of the Stone Mountain granite, distinct U, Th/U, and Ti values compared to their magmatic overgrowths. These observations are consistent both with the low diffusivity of most trace elements in zircon (e.g., Cherniak et al., 1997) and with their armoring from later fluid alteration by the magmatic overgrowths.

4.3. Zircon suites with mostly magmatic textures

Zircon suites with > 70% magmatic oscillatory zoning include the Spirit Mountain granite (MG3b), the Mirage granite (MG3a), and the younger series of San Jacinto samples (tonalite IG2; granodiorites RG1 and RG3). Among all of these analyses, LREE-I ranges 20–275 (Fig. 7), and lacks clear correlations with light elements (Fe*, Mn). LREE-I correlates instead, within units, with proxies for melt cooling and fractionation, including Ti, Hf, Th/U, and HREE/MREE (as proposed by Claiborne et al., 2010). Despite being offset to unusually high absolute

Highly altered suites (based on texture):
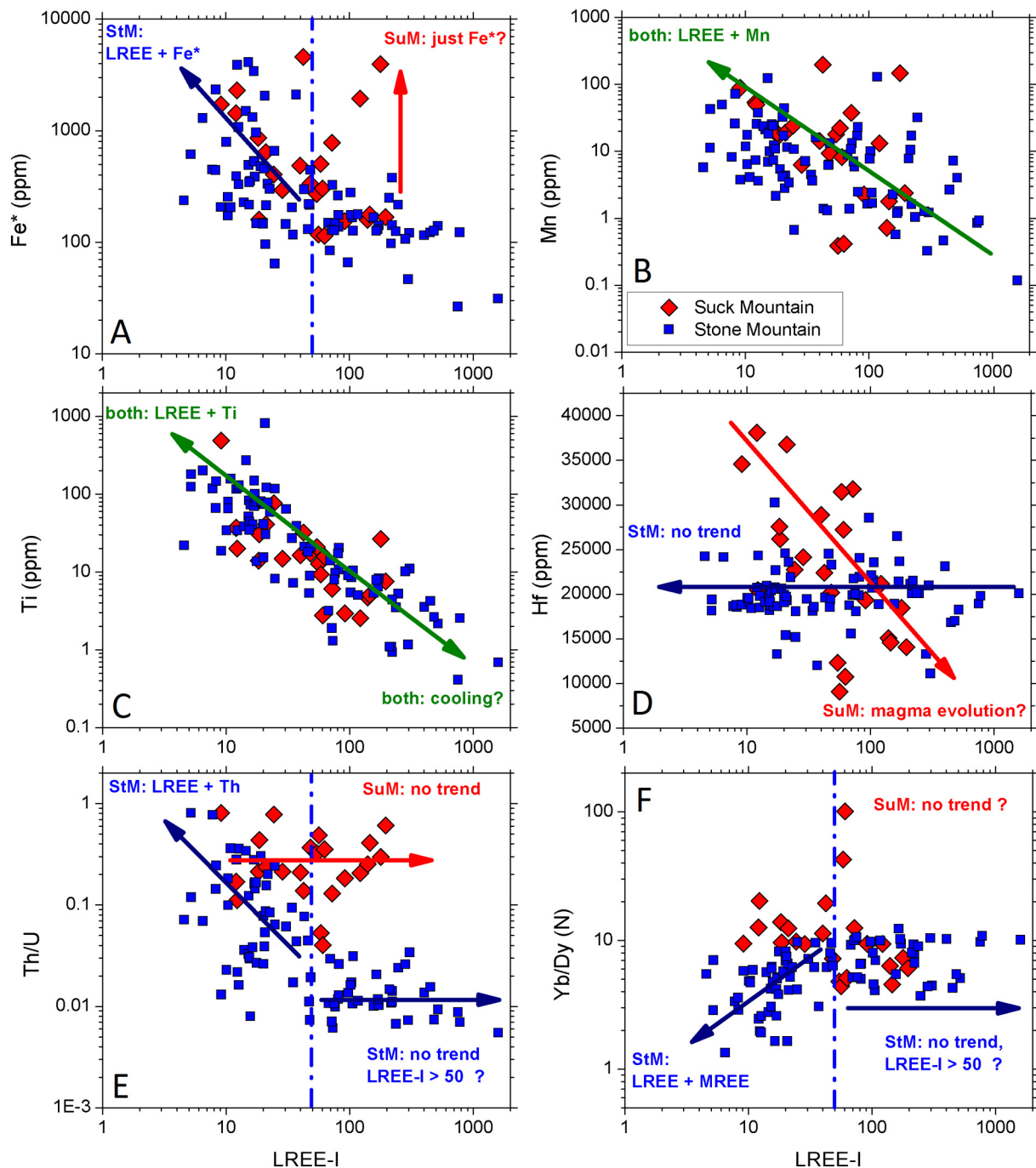
Fig. 5. Relationship between LREE-I and various contaminants in zircon from the highly altered Stone Mountain and Suck Mountain suites. A) Fe* vs LREE-I reveals increasing Fe* with lower LREE-I for LREE-I < 50; B) Mn vs LREE-I reveals contamination by Mn at low LREE-I; C) Ti vs LREE-I; this strong correlation may represent a mixture of Ti contamination at low LREE-I and melt evolution and cooling at high LREE-I; D) Hf vs LREE-I; E) Th/U vs LREE-I, in which the strong increase in Stone Mountain zircons' Th/U with lower LREE-I below LREE-I < 50 is probably due to contamination by the widespread secondary phosphates; F) Yb/Dy vs LREE-I, in which the decrease in Yb/Dy for LREE-I < 50 in Stone Mountain zircons may also represent contamination by LREE-enriched secondary phosphates.

values of Th/U (compared to most continental zircons; see e.g. Grimes et al., 2015; Burnham and Berry, 2017), zircons from the Spirit Mountain batholith also show a negative correlation between Th/U and LREE-I. Rare zircons with patchy texture show no clear evidence for trace element alteration. We interpret these zircons as potentially re-crystallized but largely chemically unaltered. A handful of zircons contain unrealistically high levels of Mg (10s–100s ppm), but most zircons contain magmatically reasonable values of Ti (e.g., Watson and

Harrison, 2005) and low Mn. No clear breaks in slope are in evidence between LREE-I and likely contaminants.

Despite its 42% patchy zoned zircon suite and evidence for deuteric fluid flow in hand sample (Walker et al., 2007) and thick section (Fig. 1b), zircon from the Spirit Mountain leucogranite ranges only as low as 28 in LREE-I, ranges only an order of magnitude in LREE-I, and shows no correlations between light element contaminants and LREE-I (see Fig. 7). Instead, LREE-I variation in the Spirit Mountain
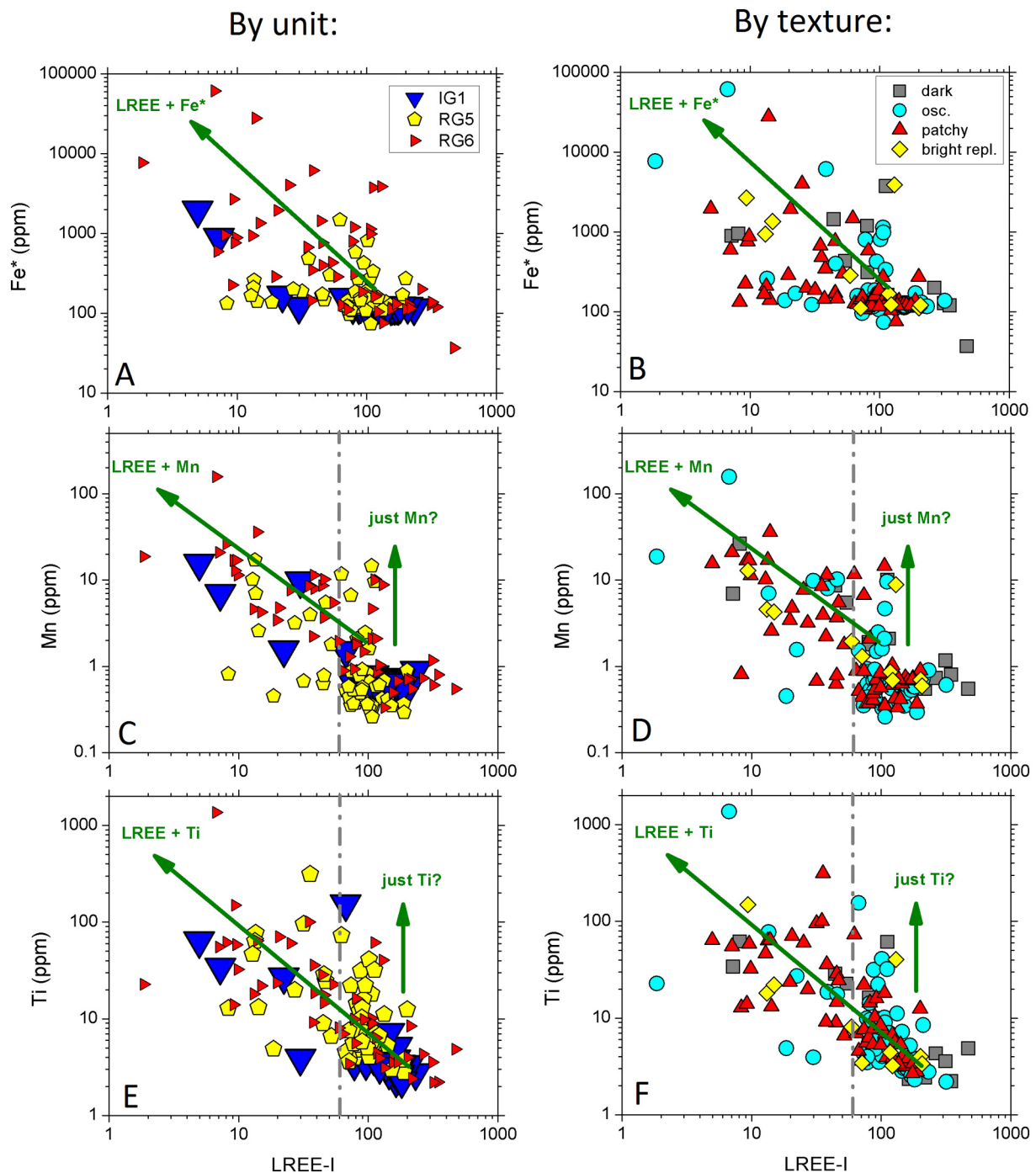
Fig. 6. Relationship between LREE-I and various contaminants in zircon from the older San Jacinto suite. A, C, E) data grouped by unit; B, D, F) data grouped by zircon CL texture. A, B) Fe* vs LREE-I reveals contamination involving higher LREE as well as Fe*; C, D) Mn vs LREE-I reveals LREE + Mn contamination as well as potential contamination by Mn without substantial LREE; E, F) Ti vs LREE-I similar to results for Mn. Samples with LREE-I > 60 appear to show negligible LREE alteration.

leucogranite appears to be driven almost entirely by melt compositional evolution, correlating closely with Hf content and the HREE/MREE ratio (as proposed by Claiborne et al., 2010).

5. Discussion

Zircon suites from the studied granitoids range from pervasively altered to apparently unaltered (see Table 2). These categories largely line up with the proportions of altered CL zoning among the zircon suites, with populations containing > 40% altered zircon also

containing a high proportion of grains with low LREE-I and high levels of likely contaminants. The populations with little evidence for alteration include the various units of the Spirit Mountain batholith and the latest, largely undisturbed intrusions of the San Jacinto Mountains (IG2 tonalite; RG1 and RG3 granodiorites). These zircons tend to display higher average LREE-I that correlates well with indicators for melt evolution, such as Hf and Th/U (Claiborne et al., 2010). Zircons from earlier plutons in the San Jacinto Mountains, as well as the pervasively altered zircons of the Stone Mountain and Suck Mountain granites, mostly lack clear relationships between LREE-I and melt evolution.

Largely unaltered suites (based on texture):
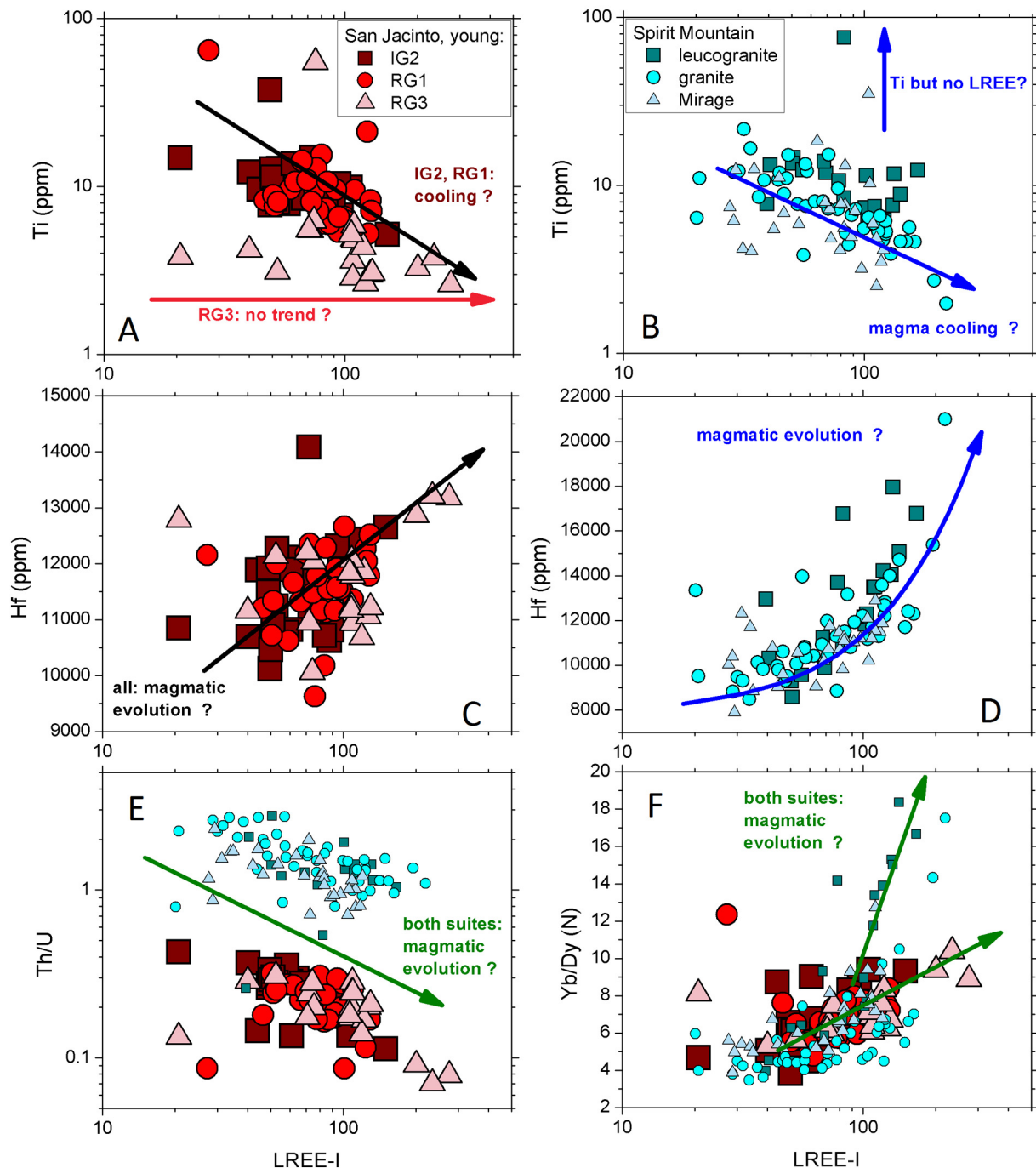
Fig. 7. Relationship between LREE-I and various indicators for magmatic evolution in zircon from the largely unaltered suites of the Spirit Mountain batholith and the younger San Jacinto granitoids. A, B) Ti vs LREE-I reveals a negative correlation expected for melt cooling; C, D) Hf vs LREE-I reveals a positive correlation expected for magmatic compositional evolution; E) Th/U vs LREE-I reveals a negative correlation expected for magmatic compositional evolution; F) Yb/Dy vs LREE-I reveals a positive correlation expected for MREE mineral fractionation (Yb/Dy standing in for HREE/MREE in general). Most units from both magmatic suites contain sphene (Walker et al., 2007; Bell et al., 2018).

However, they show clearer relationships between LREE-I and Fe*, Mn, and Ti. The less altered suites lack these strong correlations between LREE-I and contaminants. Zircons in the more pervasively altered suites also range to at least an order of magnitude lower LREE-I.

In most of the pervasively altered suites, zircon with patchy zoning or CL-bright overprinted areas are more likely to have low LREE-I and higher contents of Fe*, Mn, and Ti. However, regions of zircon with magmatic oscillatory zoning are found with LREE-I as low as 1 and with

very high levels of contamination. Pb loss as shown by U-Pb discordance shows little relationship with LREE-I, while increasing levels of common Pb contamination are evident with lower LREE-I. This is consistent with zircon chemical alteration of the type measured by the LREE-I mainly owing to contamination by later mineral phases rather than thermally induced recrystallization or diffusion, although a confounding factor in the lack of correlation between discordance and LREE-I may be the relatively low precision of SIMS U-Pb ages. Zircons

Table 2

Trace element alteration and LREE-I behavior of zircon suites investigated in this study. Note the placement of the Spirit Mountain leucogranite in sample More information on lithology, age, and setting is available in Table 1 and in electronic annex EA-1. Clear alteration to zircons: based on presence of low LREE-I values, high concentrations of light elements. Effects of LREE-I filtering: changes to trace element plots elucidating progressive melt compositional evolution (e.g., Eu/Eu* for plagioclase fractionation, Yb/Gd for sphene and hornblende fractionation).

Sample	Alteration mechanism	Clear alteration to zircons?	LREE-I influences	Minimum LREE-I	Effects of LREE-I filtering (≥ 60)
Suites with significant alteration to zircons					
Stone Mountain granite	Deuteric fluids	Many; light elements + LREE-I	Mostly contamination	5	Significant changes to interpretation
Suck Mountain granite	Uncertain	Many; light elements + LREE-I	Mostly contamination	9	Significant changes to interpretation
IG1, RG5, RG6 (old San Jacinto)	Intrusion by granitoids	Some to many; light elements + LREE-I	Mostly contamination	2	Significant changes to interpretation
Suites lacking significant alteration to zircons					
IG2, RG1, RG3 (young San Jacinto)	No mechanism obvious	Rare cases; light elements + LREE-I	Mostly melt evolution	21	Almost no change
Spirit Mountain leucogranite	Deuteric fluids	Rare cases; light elements	Melt evolution	39	Subtle changes to early melt history interpretations
Spirit Mountain granite	High-T: intrusion by granite; low-T: fault-related fluids	Rare cases; light elements + LREE-I	Melt evolution	20	Subtle changes to early melt history interpretations
Mirage granite	Fault-related fluids	None?	Melt evolution	28	Almost no change

analyzed for U-Pb age by TIMS (e.g., TIMS-TEA trace element + U-Pb age protocol of Schoene et al., 2010) might show correlations that are obscured by the low SIMS precision. For many in situ analytical protocols, including the SIMS analyses presented in this manuscript, the U-Pb and trace element analyses also sample different volumes of zircon, which may add to scatter in the relationship between U-Pb systematics and measured chemical alteration.

5.1. Expected response of LREE-I to melt evolution and contamination

Because both melt evolution and contamination by exotic materials can affect the shape of the REE pattern in zircon, expected trends need to be defined for both processes. Fig. 8a shows the partition coefficients at various temperatures of REE^{3+} ions relative to Zr^{4+} in zircon, calculated from the lattice strain formulation of Blundy and Wood (1994) using a Young's modulus of 710 GPa and a lattice site radius of 0.833 Å (parameters calculated by Burnham and Berry, 2012 to fit the partition coefficients determined by Sano et al., 2002). With decreasing temperature, the HREE/LREE partitioning increases by orders of magnitude. When this trend is coupled with the decrease in LREE/HREE of most magmas during progressive crystallization owing to the higher compatibility of LREE in most rock-forming minerals, a great deal of natural variation can be expected in magmatic zircon. Earlier crystallizing zircons will thus tend to form with lower LREE-I than zircons crystallized from the same magma at lower temperature and after further fractional crystallization, apart from any influence of contamination or alteration. As an example, Fig. 8b shows lattice strain-derived partition coefficients (calculated from the same model shown in Fig. 8a) at various temperatures applied to a melt with the composition of the average upper continental crust (Rudnick and Gao, 2003). The resulting zircon LREE-I increases with decreasing temperature. (This model does not include the effects of mineral fractionation, which will tend to enhance the increase in LREE-I with melt evolution, and so shows the minimum increase in LREE-I with decreasing melt temperature.)

Most contaminating materials will have a higher LREE/HREE ratio than zircon owing to zircon's strong preference for HREE (e.g., Hoskin and Schaltegger, 2003). Most contaminants will therefore be expected to decrease measured LREE-I along with increasing light element abundances, given that mainly silicates and oxides are present as secondary phases in zircon (Fig. 3). Apatite is also a common inclusion phase in most granitoid zircon suites (Rasmussen et al., 2011) except those originating in highly felsic granites (Bell et al., 2018), and inadvertent sampling of apatite inclusions would be expected to correlate with a large increase in measured P (as well as Ca, for protocols measuring Ca abundance). We show the expected effects of contamination of a model zircon with LREE-I = 70 and typical REE contents by materials with the composition of the average upper continental crust and a model apatite composition (Durango apatite, Frei et al., 2005; Fig. 8c). Igneous apatite's REE slope varies widely, but except for apatite from highly enriched granitic pegmatites, LREE is generally enriched over HREE (Belousova et al., 2002b). By contrast, the much higher LREE contents in monazite lead to a much more dramatic decrease in LREE-I with progressive contamination. Xenotime is also very rich in HREE, but its natural LREE/HREE ratio varies significantly. For metamorphic xenotime associated with the Jack Hills zircons, for instance, the average composition (based on results from Rasmussen et al., 2010, 2011; Bell et al., 2015) has LREE-I = 29, but LREE-I varies from 8 to 108. Thus, although only a small amount of contamination is needed to affect the LREE-I, the end results are highly dependent upon the xenotime composition (Fig. 8d). Xenotime contamination would best be detected by large increases in P and Y.

The lack of correlation of LREE-I with P in most of our zircon suites (see supplementary figures in EA-1) suggests that phosphates, either primary or secondary, do not commonly contaminate the measured REE in these suites. This contrasts with the steep increase in P with decreasing LREE-I among the Jack Hills zircons (Bell et al., 2015) owing
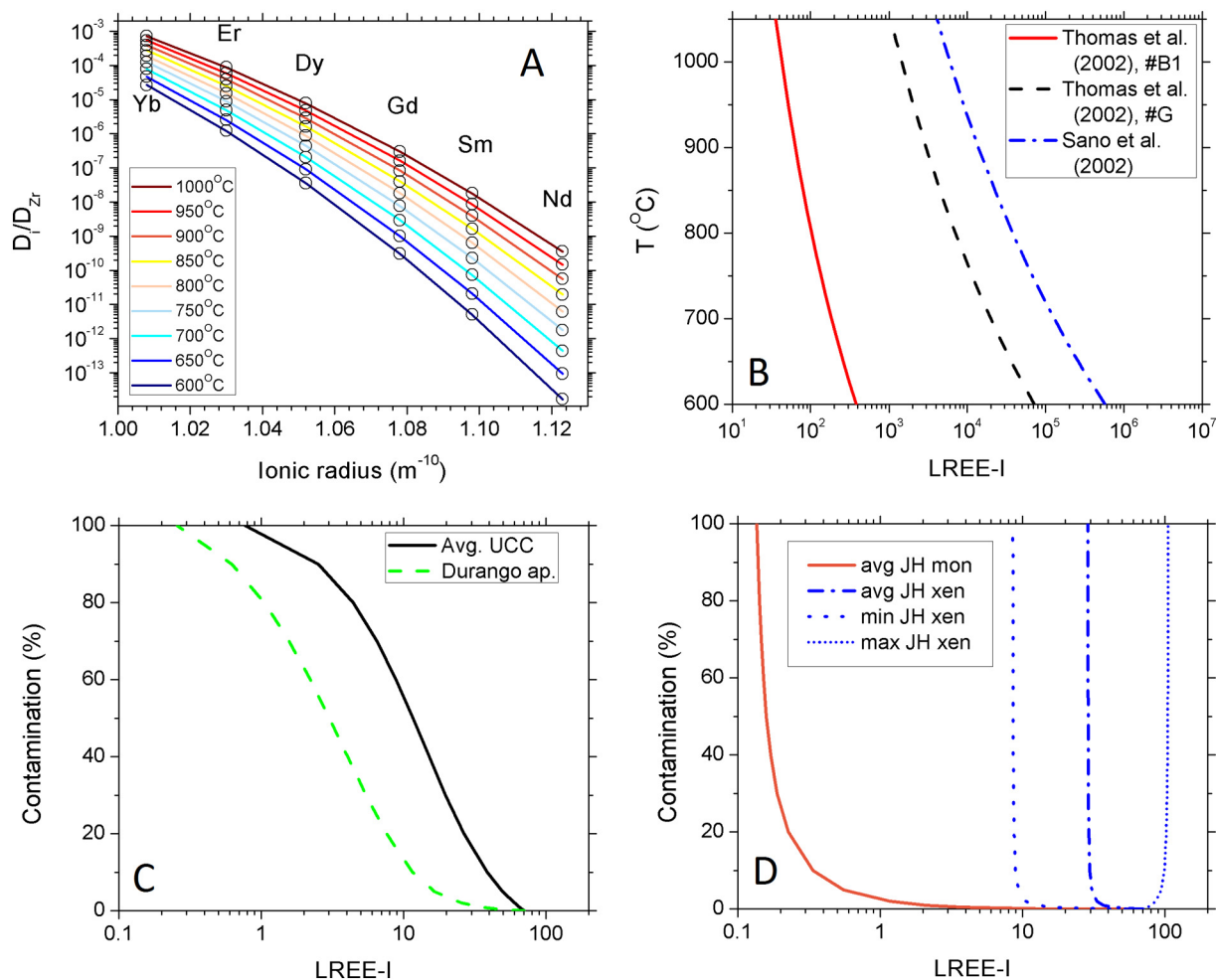
Fig. 8. Models for variation in the LREE-I with magma cooling and later contamination. A) Changing partition coefficients of REE in zircon with temperature calculated from the formulation of Blundy and Wood (1994) and using parameters calculated by Burnham and Berry (2012) for the partition coefficient observations of Sano et al. (2002). B) Expected variation in LREE-I for zircon grown in a melt with the composition of the average upper continental crust (Rudnick and Gao, 2003) at various temperatures. Different models use the parameters calculated by Burnham and Berry (2012) for the partition coefficient observations of the listed studies. C) Change in LREE-I expected for contamination of zircon with material of either the average upper continental crust composition or the composition of Durango apatite. D) Change in LREE-I expected for contamination with REE-rich phosphates monazite and xenotime. Example monazite and xenotime compositions taken from averages of metamorphic phosphates grown in the Jack Hills quartzite (Rasmussen et al., 2010, 2011; Bell et al., 2015). Monazite causes the most extreme changes in LREE-I while xenotime is more variable. Apatite and material similar to average continental crust would have similar effects volumetrically on the measured LREE-I, but apatite should also cause a large increase in P with decrease in LREE-I, which is not often recognized in our data.

to the distinct, xenotime- and monazite-rich secondary assemblage contaminating these zircons which is absent among most igneous suites in this study. Instead, among our igneous suites LREE-I correlates mostly with Mn, Ti, and Fe* (although this pattern is not universal among low-LREE-I zircons). This suggests the dominance of ferromagnesian and other secondary silicates as contaminants in most of the altered zircons. Most of the contamination we are observing is therefore probably due to the phases mobile after zircon formation, since ferromagnesian silicates and Fe oxides are over-represented among crack-filling phases.

For the largely unaltered zircon suites, zircons tend to range from 2 to 20 ppm Ti (i.e., 650–850 °C given α_{TiO2} = 1; Watson and Harrison, 2005) and vary by approximately an order of magnitude in LREE-I. Although the absolute values of expected LREE-I vary greatly with the use of different partition coefficients, an order of magnitude increase in LREE-I over a drop of 200 °C in the range of usual crustal granitoid temperatures is close to the expected model results (Fig. 8b). This likely approximates the usual behavior of LREE-I with granitoid magmatic evolution more generally.

5.2. Geologic settings more and less conducive to alteration

Zircon in granitoids that have been intruded by later magmas (older San Jacinto group; Spirit Mountain granite) or which have clear evidence for late-stage fluid circulation (Spirit Mountain leucogranite, Stone Mountain granite) are much more likely to display alteration, but the effect is not universal. In the case of intrusion by later magmas, the volume and relative timing of the later intrusion may be important factors in the two opposing cases from this study. The older generation of granitoids in the San Jacinto Mountains contains a large proportion of low-LREE-I zircons rich in Ti, Mn, and Fe* (Fig. 6) and was intruded by the ca. 80 km² scale (estimated from maps of Hill, 1984) granitoids of the younger magmas some 10 Ma (in the case of older units RG5 and IG1) or 20 Ma (in the case of older unit RG6) after their formation. On the other hand, the Spirit Mountain granite where it was intruded by (or included as pods within) the ca. 10 km² scale (estimated from map of Walker Jr et al., 2007) Mirage granite yields a zircon suite with only slight evidence for alteration (Fig. 7), and their separation in time is perhaps 1 Ma (Walker Jr et al., 2007; Bell et al., 2018) – potentially before full solidification of the earlier Spirit Mountain granite given the

batholith's protracted construction (Walker Jr et al., 2007).

Both the Stone Mountain granite and the Spirit Mountain leucogranite contain mineralogic evidence for late-stage fluid flow (Longfellow and Swanson, 2011; Walker Jr et al., 2007), but Stone Mountain contains mostly altered zircon while the extent of alteration in Spirit Mountain leucogranite zircon is much lower. In the case of Stone Mountain, the very U-rich (typically 1000–10,000 ppm) zircon would have been very susceptible to alteration over the subsequent metamorphic history of the Appalachian Inner Piedmont during Alleghanian collision, which extends to at least 268 Ma (Dallmeyer et al., 1986; Hatcher, 1987) in addition to any deuteric fluids associated with the late stages of pluton crystallization. Spirit Mountain leucogranite zircons on the other hand contain only several 100 s ppm U and formed only at 16 Ma (Walker Jr et al., 2007), being subsequently unroofed during Basin and Range extension (e.g., Haapala et al., 2005).

5.3. Contamination vs magma evolution

The vast majority of zircons which are rich in Mn, Ti, and Fe* are also low in LREE-I. In suites with a high proportion of non-magmatic CL textures and contaminant-rich zircons, LREE-I noticeably correlates with these likely contaminant materials for LREE-I < 40. LREE-I correlates strongly either with light elements at low LREE-I or with indicators for magma compositional evolution at high LREE-I. For suites poor in altered zircons (e.g., Spirit Mountain and Mirage units; younger San Jacinto units), the correlation of LREE-I with magma compositional evolution are evident through most of the range of LREE-I, unobscured by the contamination seen in the other suites.

A handful of zircon in some suites (notably, Suck Mountain and the older San Jacinto granitoids) with high LREE-I and otherwise magmatic-seeming textures display high contents of light elements, including Ti contents pointing to unrealistically high crystallization temperatures (e.g., Harrison et al., 2007). A potential explanation is that these zircons are contaminated by oxide phases (Fe, Ti, Mn) that didn't include appreciable REE, unlike the majority of contaminants which are probably dominated by silicates based on the prevailing inclusion assemblages for the zircons. Two of the older San Jacinto units are on the high end of Fe-Ti oxide content in the inclusion assemblage (5% and 7% with an average over all units studied by Bell et al., 2018 of 3.7 ± 2.9%). However, this behavior seems to be the exception rather than the rule. These high-Mn, Ti, and Fe* zircons fall outside the main trend of decreasing Ti with increasing LREE-I, suggesting that samples falling significantly outside such trends should also be screened as likely altered.

5.4. LREE-I filtering strategies

For Stone Mountain zircons, contaminants appear to dominate the trace element signature at values below LREE-I~50. The older San Jacinto suite has less systematic contaminant behavior but trace element signatures above LREE-I~60 (and lacking anomalously high Mn and Ti levels) are probably primary. The low number of Suck Mountain analyses may impede the identification of similar signatures, while the lack of pervasive textural alteration and predominance of higher LREE-I values among the other zircon suites means alteration signals aren't well developed. Using this guideline, we conservatively filter the zircon suites for samples with LREE-I > 60 and present the results in Figs. 9 and 10. For the highly altered zircons of the Stone Mountain granite, altered zircons range to unrealistically high apparent crystallization temperatures (> 1000 °C) (Fig. 9a). Eu/Eu* decreases with temperature, as expected for plagioclase fractionation, but which variations are due to contamination is unclear without reference to the LREE-I. The filtered dataset consists of a restricted, more realistic temperature range and clarifies the true extent of variation in Eu/Eu* among primary zircon compositions. The very low Th/U values (for LREE-I < 60, Th/U averages ca. 0.014) for Stone Mountain zircon are anomalous even
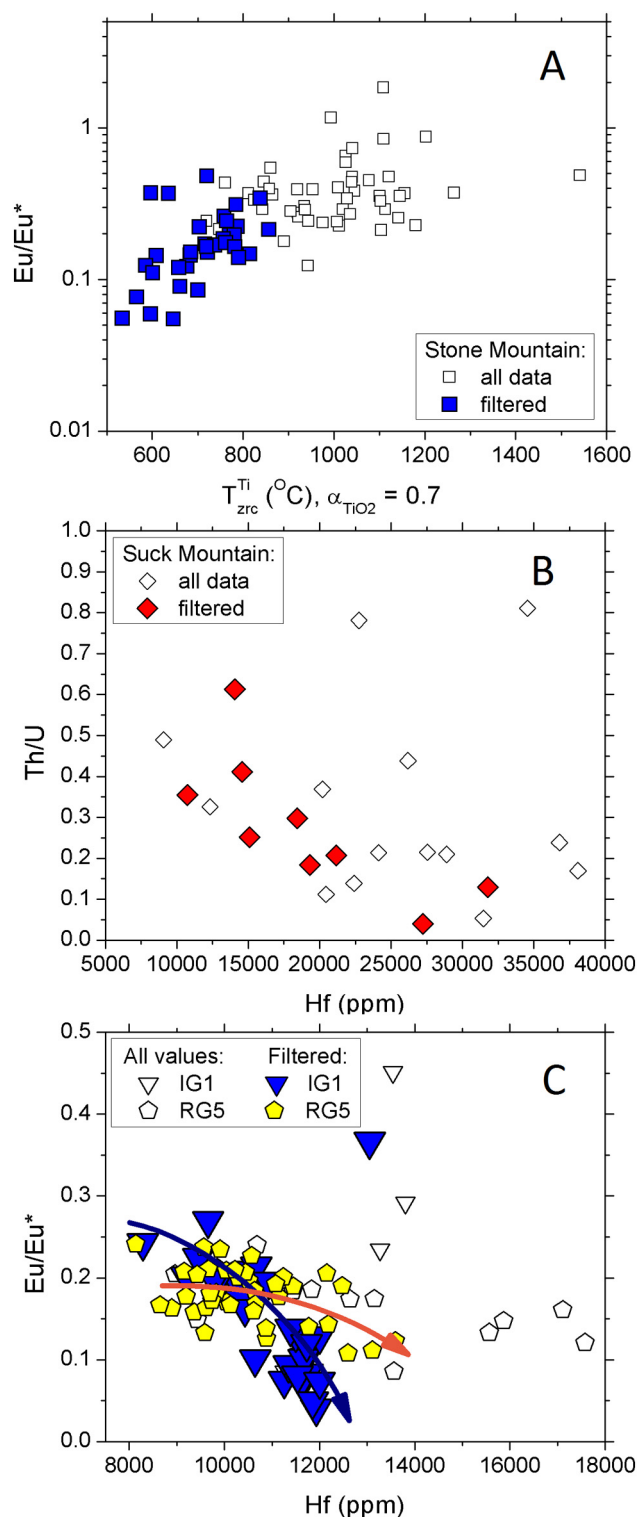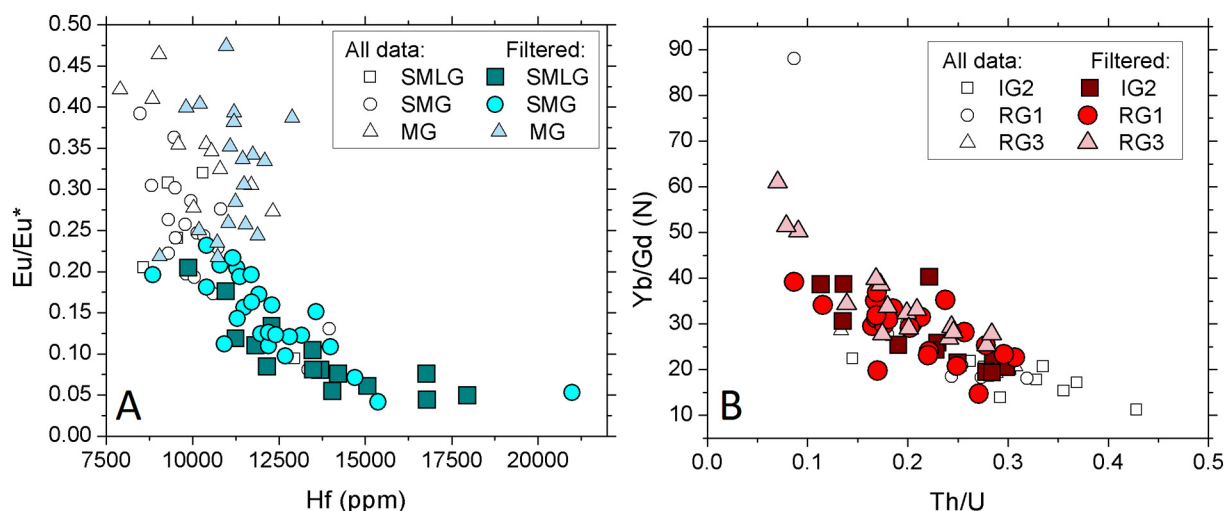

Fig. 9. Application of the LREE-I filter to the highly altered zircons of the Stone Mountain (A), Suck Mountain (B), and older San Jacinto (C) granitoids clarifies fractionation trends for plagioclase in Stone Mountain (A) and the older San Jacinto units (C) and reveals the expected decrease in Th/U with melt evolution and cooling for Suck Mountain (B).

for S-type granites (e.g., Burnham and Berry, 2017), and even assuming a relatively low $\alpha_{TiO2} = 0.3$, many of their apparent crystallization temperatures are subsolidus (relative even to a water-saturated solidus; ranging to 587 °C for $\alpha_{TiO2} = 0.3$). However, the high boron content of the system as shown by the extensive tourmaline developed during late-

Fig. 10. Application of a conservative LREE-I filter to suites with little evidence for alteration. Filtering out samples with LREE-I < 60 results in negligible changes to interpretations of the early melt history. A) Samples from the Spirit Mountain batholith; B) samples from the youngest pulse of San Jacinto granitoids.

stage fluid circulation (Longfellow and Swanson, 2011) may have lowered the solidus temperature significantly. Alteration of zircon in the Suck Mountain granite (Fig. 9b) appears to obscure the relationship between Th/U melt evolution (with melt evolution shown by Hf content; Claiborne et al., 2010). However, filtering for samples with LREE-I > 60 reveals the expected decrease in Th/U with increasing Hf. Applying the LREE-I > 60 filter clarifies the decrease in Eu/Eu* with melt evolution due to plagioclase fractionation in the RG5 quartz diorite and especially the IG1 granite (Fig. 9c).

Despite the promise of LREE-I filtering in revealing magmatic compositional trends in partially altered zircon suites, some zircons in the largely unaltered late San Jacinto and Spirit Mountain suites range to well below LREE-I < 60 without clear evidence for contamination by Mn, Ti, and Fe*, raising the question of whether zircons with low LREE-I may arise naturally without alteration. If they can, then applying a filter runs the risk of discarding potentially interesting and useful samples from early, less compositionally evolved magmas. For the present dataset, our conservative filtering for LREE-I > 60 has slight effects on interpretations of magma compositional evolution. Somewhat fewer low-Hf, high-Eu/Eu* zircons from Spirit Mountain units are left in the filtered dataset (Fig. 10a), while applying the filter to the young San Jacinto units results in almost no change in trends but only removes some samples from the higher-Th/U, lower-Yb/Gd region of the trend (Fig. 10b). For zircon suites with significant alteration, any naturally low-LREE-I samples are unlikely to be distinguishable from altered zircons. However, based on these samples we tentatively conclude that applying the filter and potentially excluding these samples has minimal effects on the interpretation of unaltered zircon suites.

5.5. The necessity of alteration filtering for detrital zircon provenance schemes

There is considerable interest in developing trace element-based provenance schemes for detrital zircon (e.g., Hoskin and Ireland, 2000; Belousova et al., 2002a; Grimes et al., 2007, 2015; Burnham and Berry, 2017). However, apart from the trace elements that have been demonstrated to quantitatively correspond to magmatic temperature (Ti; Watson and Harrison, 2005) and oxygen fugacity (Ce/Ce*; Trail et al., 2011), the efficacy of the lanthanide and actinide elements for discriminating various provenances is debatable. Hoskin and Ireland (2000) point out the similarity of most terrestrial zircon REE patterns and find little variation among various crustal rock types. However, Grimes et al. (2007) demonstrate that zircons of oceanic versus continental affinity can be distinguished using a discriminant plot of U/Yb

vs. Y. Grimes et al. (2015) present a discriminant scheme using various ratios of the elements U, Nb, Sc, Yb, Gd, and Ce to distinguish among zircons from magmatic arcs, oceanic islands, and mid-ocean ridges. Focusing more closely on continental lithologies, Belousova et al. (2002a) suggest a detailed discriminant scheme based on various classification trees determined from extensive ICPMS analyses of zircon from diverse igneous rock types both rare and common. Finally, Burnham and Berry (2017) suggest that the (REE + Y)/P ratio discriminates between zircon from S- and I-type granitoids (Chappell and White, 1974), with the peraluminous nature of S-type granitoids meaning that apatite will not saturate (Pichavant et al., 1992) and thus P will be available in higher abundance, substituting into zircon predominantly by the xenotime substitution $REE^{3+} + P^{5+} \longleftrightarrow Zr^{4+} + Si^{4+}$ (e.g., Hoskin and Schaltegger, 2003). However, they demonstrate that metaluminous I-type granitoids tend to yield a higher proportion of zircon with (REE + Y)/P > 1, reflecting other substitution mechanisms (potentially involving H^+; De Hoog et al., 2014).

Any trace element-based provenance scheme for detrital zircon is premature without a reliable tool for filtering zircon datasets to exclude measured values which reflect alteration or incorporation of inclusions rather than original zircon chemistry. As the present study demonstrates, even zircon with magmatic oscillatory zoning can yield altered abundances due to incorporation of phases deposited during high-temperature fluid flow. Although not all cracks will be associated with contamination, avoiding cracks is a good first order strategy for avoiding chemical alteration. However, this is not always possible even with careful in situ analysis. Ion microprobe analyses have the best chance of avoiding such features due to their relatively small depths of ablation, but often for highly cracked grains this will not be possible. Avoiding contamination based on textural indicators becomes even more difficult with LA-ICPMS, because although modern laser ablation systems can make measurements with increasingly small spot size, the analysis pit will typically be several microns to 10 s of microns deep and could intersect unseen cracks and inclusions within the volume of the zircon. For methods such as solution ICP-MS or TIMS-TEA (in which the same volume of zircon dissolved for a TIMS U-Pb age is measured for trace elements by solution ICP-MS; Schoene et al., 2010), the problem also pertains, especially for cracks and clear inclusions not perceptible by visual microscopy. Primary inclusions not in contact with cracks will not be removed by chemical abrasion procedures and also remain a potential contaminant for TIMS-TEA measurements.

Results from the present study are all taken from well-understood magmatic systems where the parent rock is available for inspection. The necessity of an alteration filter is even clearer for detrital grains lacking

constraints on pre-depositional history. For metasediments the effects of metamorphism since deposition are also important, as shown by the partially altered suite of Hadean zircons at Jack Hills, Western Australia (Hoskin, 2005; Bell et al., 2016). Various proposed provenance methods will be affected to varying degrees by the most common patterns of chemical alteration to zircon. The method of Grimes et al. (2007) is less likely to be susceptible to zircon alteration, since it relies on the quantities Yb/U, Y, and Hf. Although U is a common contaminant in the Jack Hills detrital zircons, it does not seem to be a very common contaminant in the igneous zircons in the present study and the extent of U contamination may be situationally dependent on host rocks which contain xenotime or other U-rich phases. Y is also likely to be a contaminant also only in situations where secondary xenotime is abundant. Because Ce is an LREE, methods employing it (such as Grimes et al., 2015) may also be susceptible to misinterpretation. Because contamination with LREE-rich material will greatly increase the (REE + Y)/P of a measured volume of zircon, the provenance method of Burnham and Berry (2017) for distinguishing S- vs I-type origins also requires careful screening.

Careful screening of training datasets is also of paramount importance in building usable provenance methods. The discriminant diagrams of Belousova et al. (2002a) for instance rely on several quantities that are often heavily affected by contamination, including U, Th/U, and the HREE/LREE slope. Inspection of their average Ti quantities for several granitoid compositional classes which formed the basis for their provenance scheme reveals unrealistically high concentrations (see Harrison et al., 2007) of hundreds to thousands of ppm. A portion of the zircon populations included in the training set for these discriminant trees must therefore have undergone alteration. Given the near certainty that the HREE/MREE, U, and Th/U of these grains were also altered, the reliability of this provenance scheme is highly questionable.

5.6. Applying the LREE-I to natural zircon populations

The best strategies for employing the LREE-I to filter zircon suites for chemical alteration will differ based on the populations under study. Because cogenetic suites of zircon, as in a single pluton or batholith, are likely to share many aspects of their alteration history, they are more likely to present breaks in slope or other changes in behavior between LREE-I and light element contaminants at a particular LREE-I value that point to the index value below which alteration signals dominate (e.g., LREE-I = 50 for Stone Mountain granite and, conservatively, 60 for the older San Jacinto granitoids). Detrital zircon from metasediments such as the Jack Hills meta-conglomerate are also likely to show coherent alteration behavior due to shared metamorphic history (e.g., Bell et al., 2016). For these populations, LREE-I values below which alteration dominates should first be estimated and a modified filter based on this value applied to the zircon data before interpreting it in terms of magmatic compositions.

However, low-temperature fluid flow and diagenesis is unlikely to impose such a coherent alteration signal on detrital zircon in unmetamorphosed sediments. Individual detrital zircons may well have experienced hydrothermal alteration before their deposition in the sediment, and zircon from many different magmatic systems may be incorporated into a single detrital population, making the chances of coherent relationships between LREE-I and indicators for melt evolution unlikely. For detrital zircon in unmetamorphosed sediments that lack clear changes in contaminant behavior at lower LREE-I, the best strategy is to filter for zircon with a conservative LREE-I (potentially 60), based on the contaminant behavior identified in this study. A cautious approach should be taken in interpreting the rare samples with high LREE-I but unrealistically high contents of Ti. High Ti contents that do not follow a population's general trend (especially when correlated with high contents of Mn and Fe) with LREE-I are probably due to contamination with oxides that might have a low enough REE

content to not affect the LREE-I. Similarly, samples with low LREE-I but reasonable Ti temperatures may display either alteration or true magmatic signatures, but their exclusion from the interpreted dataset will in most cases not result in large differences to interpretations (e.g., Fig. 10).

6. Conclusions

The shape of the REE pattern in zircon as quantified by the light rare earth element index (LREE-I) tracks contamination by secondary phases included during zircon alteration, with the vast majority of unaltered zircon falling above LREE-I > 50 or 60 and mostly altered zircons falling below LREE-I < 50, as identified by breaks in slope in the relationships between the LREE-I and various contaminants in highly altered zircon populations. CL imaging for magmatic zoning appears to be a less efficient means of selecting zircon for trace element analysis: primary, oscillatory chemical zoning patterns are more common among zircon with unaltered LREE-I, but some oscillatory zoned samples range to LREE-I as low as 1 and contain other chemical contaminants. Zircons with patchy zoning are found throughout the range of LREE-I and light element contamination and probably represent recrystallization with or without chemical contamination. The LREE-I is particularly useful in filtering altered from magmatic compositions in highly altered zircon populations, such as those altered during intrusion of later magmas or during deuteric circulation in a crystallizing pluton. Filtering in this case helps to reveal magmatic compositional variations related to mineral fractionation (e.g., Yb/Gd, Eu/Eu*) that are otherwise obscured by later alteration. The LREE-I is applicable to zircon in a wide range of magmatic systems as well as detrital populations, in which case we suggest using a conservative filtervalue of LREE-I > 60 as delineating unaltered magmatic trace element signatures. The LREE-I filter becomes more crucial with increasing volume of material consumed during analysis (e.g., solution methods, or laser ablation with a deep pit), since hidden cracks and inclusions may dominate the trace element signatures without leaving visible evidence in the analyzed zircon.

Appendix A. Supplementary data

Supplementary data to this article can be found online at https://doi.org/10.1016/j.chemgeo.2019.02.027.

References

Barboni, M., Boehnke, P., Schmitt, A.K., Harrison, T.M., Shane, P., Bouvier, A.S., Baumgartner, L., 2016. Warm storage for arc magmas. Proc. Natl. Acad. Sci. 113, 13959–13964.

Barth, A.P., Wooden, J.L., Jacobson, C.E., Economos, R.C., 2013. Detrital zircon as a proxy for tracking the magmatic arc system: the California arc example. Geology 41, 223–226.

Bell, E.A., Boehnke, P., Hopkins-Wielicki, M.D., Harrison, T.M., 2015. Distinguishing primary and secondary inclusion assemblages in Jack Hills zircons. Lithos 234, 15–26.

Bell, E.A., Boehnke, P., Harrison, T.M., 2016. Recovering the primary geochemistry of Jack Hills zircons through quantitative estimates of chemical alteration. Geochim.

Cosmochim. Acta 191, 187–202.

Bell, E.A., Boehnke, P., Harrison, T.M., Wielicki, M.M., 2018. Mineral inclusion assemblage and detrital zircon provenance. Chem. Geol. 477, 151–160.

Belousova, E., Griffin, W.L., O'Reilly, S.Y., Fisher, N.L., 2002a. Igneous zircon: trace element composition as an indicator of source rock type. Contrib. Mineral. Petrol. 143, 602–622.

Belousova, E.A., Griffin, W.L., O'Reilly, S.Y., Fisher, N.I., 2002b. Apatite as an indicator mineral for mineral exploration: trace-element compositions and their relationship to host rock type. J. Geochem. Explor. 76, 45–69.

Blundy, J., Wood, B., 1994. Prediction of crystal–melt partition coefficients from elastic moduli. Nature 372, 452.

Blundy, J., Wood, B., 2003. Partitioning of trace elements between crystals and melts. Earth Planet. Sci. Lett. 210, 383–397.

Burnham, A.D., Berry, A.J., 2012. An experimental study of trace element partitioning between zircon and melt as a function of oxygen fugacity. Geochim. Cosmochim. Acta 95, 196–212.

Burnham, A.D., Berry, A.J., 2017. Formation of Hadean granites by melting of igneous crust. Nat. Geosci. 10, 457.

Cavosie, A.J., Valley, J.W., Wilde, S.A., 2006. Correlated microanalysis of zircon: trace element, δ18O, and U–Th–Pb isotopic constraints on the igneous origin of complex > 3900 Ma detrital grains. Geochim. Cosmochim. Acta 70, 5601–5616.

Chappell, B.W., White, A.J.R., 1974. Two contrasting granite types. Pac. Geol. 8, 173–174.

Cherniak, D.J., Watson, E.B., 2001. Pb diffusion in zircon. Chem. Geol. 172, 5–24.

Cherniak, D.J., Hanchar, J.M., Watson, E.B., 1997. Rare-earth diffusion in zircon. Chem. Geol. 134, 289–301.

Claiborne, L.L., Miller, C.F., Wooden, J.L., 2010. Trace element composition of igneous zircon: a thermal and compositional record of the accumulation and evolution of a large silicic batholith, Spirit Mountain, Nevada. Contrib. Mineral. Petrol. 160, 511–531.

Compston, W.T., Pidgeon, R.T., 1986. Jack Hills, evidence of more very old detrital zircons in Western Australia. Nature 321, 766.

Dallmeyer, R.D., Wright, J.E., SECOR, J.R., T, D., Snoke, A.W., 1986. Character of the Alleghanian orogeny in the southern Appalachians: Part II. Geochronological constraints on the tectonothermal evolution of the eastern Piedmont in South Carolina. Geol. Soc. Am. Bull. 97, 1329–1344.

De Hoog, J.C.M., Lissenberg, C.J., Brooker, R.A., Hinton, R., Trail, D., Hellebrand, E., 2014. Hydrogen incorporation and charge balance in natural zircon. Geochim. Cosmochim. Acta 141, 472–486.

Ferry, J.M., Watson, E.B., 2007. New thermodynamic models and revised calibrations for the Ti-in-zircon and Zr-in-rutile thermometers. Contrib. Mineral. Petrol. 154, 429–437.

Fokin, M.A., 2003. Space-Time Analysis of Magmatism: Evidence for a Early Cryogenian Plume Track in Eastern Laurentia (M.S. thesis). Virginia Tech.

Frei, D., Harlov, D., Dulski, P.E.T.E.R., Ronsbo, J., 2005. Apatite from Durango (Mexico)-a potential standard for in situ trace element analysis of phosphates. Geochim. Cosmochim. Acta 69, A794.

Geisler, T., Pidgeon, R.T., Kurtz, R., Van Bronswijk, W., Schleicher, H., 2003. Experimental hydrothermal alteration of partially metamict zircon. Am. Mineral. 88, 1496–1513.

Glover, L.I.I.I., Speer, J.A., Russell, G.S., Farrar, S.S., 1982. Ages of regional metamorphism and ductile deformation in the central and southern Appalachians. Lithos 16, 223–245.

Grimes, C.B., John, B.E., Kelemen, P.B., Mazdab, F.K., Wooden, J.L., Cheadle, M.J., ... Schwartz, J.J., 2007. Trace element chemistry of zircons from oceanic crust: a method for distinguishing detrital zircon provenance. Geology 35, 643–646.

Grimes, C.B., Wooden, J.L., Cheadle, M.J., John, B.E., 2015. "Fingerprinting" tectonomagmatic provenance using trace elements in igneous zircon. Contrib. Mineral. Petrol. 170 (46).

Haapala, I., Rämö, O.T., Frindt, S., 2005. Comparison of Proterozoic and Phanerozoic rift-related basaltic-granitic magmatism. Lithos 80, 1–32.

Harrison, T.M., Watson, E.B., Aikman, A.B., 2007. Temperature spectra of zircon crystallization in plutonic rocks. Geology 35, 635–638.

Harrison, T.M., Bell, E.A., Boehnke, P., 2017. Hadean zircon petrochronology. Rev. Mineral. Geochem. 83, 329–363.

Hatcher Jr., R.D., 1987. Tectonics of the southern and central Appalachian internides. Annu. Rev. Earth Planet. Sci. 15, 337–362.

Hildebrand, R.S., Whalen, J.B., 2017. The tectonic setting and origin of Cretaceous Batholiths within the North American Cordillera: the case for slab failure magmatism and its significance for crustal growth. Geol. Soc. Am. Spec. Pap. 532 (Geological Society of America).

Hill, R.I., 1984. Petrology and Petrogenesis of Batholithic Rocks, San Jacinto Mountains, Southern California (Ph.D. thesis). California Institute of Technology.

Hill, R.I., 1988. San Jacinto intrusive complex: 1. Geology and mineral chemistry, and a

model for intermittent recharge of tonalitic magma chambers. J. Geophys. Res. Solid Earth 93, 10325–10348.

Hoskin, P.W., 2005. Trace-element composition of hydrothermal zircon and the alteration of Hadean zircon from the Jack Hills, Australia. Geochim. Cosmochim. Acta 69, 637–648.

Hoskin, P.W.O., Black, L.P., 2000. Metamorphic zircon formation by solid-state recrystallization of protolith igneous zircon. J. Metamorph. Geol. 18, 423–439.

Hoskin, P.W., Ireland, T.R., 2000. Rare earth element chemistry of zircon and its use as a provenance indicator. Geology 28, 627–630.

Hoskin, P.W.O., Kinny, P.D., Wyborn, B., Chappell, B.W., 2000. Identifying accessory mineral saturation during differentiation of granitoid magmas: an integrated approach. J. Pet. 41, 1365–1396.

Hoskin, P.W., Schaltegger, U., 2003. The composition of zircon and igneous and metamorphic petrogenesis. Rev. Mineral. Geochem. 53, 27–62.

Longfellow, K.M., Swanson, S.E., 2011. Skeletal tourmaline, undercooling, and crystallization history of the Stone Mountain granite, Georgia, USA. Can. Mineral. 49, 341–357.

Paces, J.B., Miller, J.D., 1993. Precise U-Pb ages of Duluth complex and related mafic intrusions, northeastern Minnesota: Geochronological insights to physical, petrogenetic, paleomagnetic, and tectonomagmatic processes associated with the 1.1 Ga midcontinent rift system. J. Geophys. Res. Solid Earth 98, 13997–14013.

Pearce, J.A., Harris, N.B., Tindle, A.G., 1984. Trace element discrimination diagrams for the tectonic interpretation of granitic rocks. J. Pet. 25, 956–983.

Pichavant, M., Montel, J.M., Richard, L.R., 1992. Apatite solubility in peraluminous liquids: experimental data and an extension of the Harrison-Watson model. Geochim. Cosmochim. Acta 56, 3855–3861.

Quidelleur, X., Grove, M., Lovera, O.M., Harrison, T.M., Yin, A., Ryerson, F.J., 1997. The thermal evolution and slip history of the Renbu Zedong thrust, southeastern Tibet. J. Geophys. Res. 102, 2659–2679.

Rankin, D.W., 1975. The continental margin of eastern North America in the southern Appalachians: the opening and closing of the proto-Atlantic Ocean. Am. J. Sci. 275, 298–336.

Rasmussen, B., Fletcher, I.R., Muhling, J.R., Wilde, S.A., 2010. In situ U–Th–Pb geochronology of monazite and xenotime from the Jack Hills belt: Implications for the age of deposition and metamorphism of Hadean zircons. Precambrian Res. 180, 26–46.

Rasmussen, B., Fletcher, I.R., Muhling, J.R., Gregory, C.J., Wilde, S.A., 2011. Metamorphic replacement of mineral inclusions in detrital zircon from Jack Hills, Australia: implications for the Hadean Earth. Geology 39, 1143–1146.

Robinson, M.S., 1976. Paleozoic metamorphism of the Piedmont-Blue Ridge boundary region in west-central Virginia: evidence from K–Ar dating. Geol. Soc. Am. Abstr. Programs 8, 257–258.

Rubatto, D., Gebauer, D., 2000. Use of cathodoluminescence for U-Pb zircon dating by ion microprobe: some examples from the Western Alps. In: Cathodoluminescence in Geosciences. Springer, Berlin, Heidelberg, pp. 373–400.

Rudnick, R.L., Gao, S., 2003. Composition of the continental crust. Treat. Geochem. 3, 659.

Sano, Y., Terada, K., Fukuoka, T., 2002. High mass resolution ion microprobe analysis of rare earth elements in silicate glass, apatite and zircon: lack of matrix dependency. Chem. Geol. 184, 217–230.

Schmitt, A.K., Vazquez, J.A., 2006. Alteration and remelting of nascent oceanic crust during continental rupture: evidence from zircon geochemistry of rhyolites and xenoliths from the Salton Trough, California. Earth Planet. Sci. Lett. 252, 260–274.

Schoene, B., Latkoczy, C., Schaltegger, U., Günther, D., 2010. A new method integrating high-precision U–Pb geochronology with zircon trace element analysis (U–Pb TIMS-TEA). Geochim. Cosmochim. Acta 74 (24), 7144–7159.

Sinha, A.K., 1976. Timing of metamorphic and igneous events in the Central Piedmont and Blue Ridge. Geol. Soc. Am. Abstr. Programs 8, 267.

Trail, D., Watson, E.B., Tailby, N.D., 2011. The oxidation state of Hadean magmas and implications for early Earth's atmosphere. Nature 480, 79.

Walker Jr., B.A., Miller, C.F., Claiborne, L.L., Wooden, J.L., Miller, J.S., 2007. Geology and geochronology of the Spirit Mountain batholith, southern Nevada: Implications for timescales and physical processes of batholith construction. J. Volcanol. Geotherm. Res. 167, 239–262.

Watson, E.B., Harrison, T.M., 2005. Zircon thermometer reveals minimum melting conditions on earliest Earth. Science 308, 841–844.

Whitney, J.A., Jones, L.M., Walker, R.L., 1976. Age and origin of the Stone Mountain granite, Lithonia district, Georgia. Geol. Soc. Am. Bull. 87, 1067–1077.

Wiedenbeck, M., Hanchar, J.M., Peck, W.H., Sylvester, P., Valley, J., Whitehouse, M., ... Franchi, I., 2004. Further characterisation of the 91500 zircon crystal. Geostand. Geoanal. Res. 28, 9–39.

Wright, N.P., 1966. Mineralogic variation in the Stone Mountain granite, Georgia. Geol. Soc. Am. Bull. 77, 207–210.